

# CO<sub>2</sub>-sequestering ability of M20 grade concrete with bio-char and iron ore tailing powder

A. Sumil Kumaran<sup>1</sup> and S. Judes Sujatha<sup>2\*</sup>

<sup>1</sup>Assistant Professor, Department of Civil Engineering, Francis Xavier Engineering College, Tirunelveli – 627003, India.

<sup>2</sup>Assistant Professor, Department of Civil Engineering, University College of Engineering, Nagercoil – 629004, India

Received: 26/06/2024, Accepted: 13/11/2024, Available online: 20/11/2024

\*to whom all correspondence should be addressed: e-mail: judessuja2@gmail.com

<https://doi.org/10.30955/gnj.006314>

## Graphical abstract



## Abstract

The research aims to investigate the CO<sub>2</sub>-sequestering ability of M20 grade concrete with biochar and Iron ore Tailing Powder (ITP). The biochar was prepared by slow pyrolysis of corn stover. The obtained biochar were categorised in two series as untreated biochar and biochar subjected to pre-treatment by heating until it catches fire. The fine aggregate in the concrete was replaced with biochar at 0%, 5%, 10% and 15%. The iron ore tailing powder obtained by crushing and sieving of iron ore waste products. The cement was replaced with ITP at 0%, 25% and 50% by its weight. Water to binder ratio was maintained at 0.45, the workability of the concrete was maintained with the help of super plasticizer. The compressive strength test, CO<sub>2</sub> uptake, porosity and mercury intrusion porosimetry test were conducted to understand the effect of biochar and ITP in concrete. The test result indicate that the mix containing pre-treated biochar with 25% ITP substitution has the maximum CO<sub>2</sub> sequestration capacity without compromising its strength characteristics.

**Keywords:** Biochar, CO<sub>2</sub> sequestration, iron ore tailing powder, porosity, corn stover

## 1. Introduction

In any type of building the comparatively most occupied parts are concrete [Xuan Mao *et al.* 2018]. Few novel building materials try to replace the composition of

concrete [Palaniappan *et al.* 2022]. In the next three decades, the building sector is projected to produce 80 billion tons concrete per year [Al Khazaleh *et al.* 2022]. Studies report that about 7% of anthropogenic carbon dioxide production results from cement manufacture [Al-khazaleh and Kumar 2023]. The concrete research communities are in an urge to improve the CO<sub>2</sub> absorption property of concrete using biochar as a potential admixture [Gupta *et al.* 2018].

Biochar is a carbon-rich material produced during pyrolysis process. Biochar produced by burning 1T of agricultural waste can absorb approximately 0.8T of CO<sub>2</sub> in the atmosphere [Roberts *et al.* 2010]. The biochar are amorphous crystalline structured, which has high water holding capacity, resulting in high internal curing of concrete. Hence many researchers reported the influence of biochar on strength and toughness characteristics of concrete [Aprianti *et al.* 2015]. Few studies report that the utilization of biochar in construction industry can improves the CO<sub>2</sub> sequestration property [Ahmad *et al.* 2015]. Fracture and rupture modulus improvement, reduction in crack development of cement mortar was improved with biochar addition [Restuccia *et al.* 2017]. Few researchers explored the structural benefits of biochar in concrete along with its CO<sub>2</sub> sequestration characteristics [Kua *et al.* 2019]. These biochar were replaced with cement to estimate its pozzolanic characteristics in the concrete, the study proved the micro filler effect of biochar helped to achieve the target strength of concrete. further it improves the durability of the concrete [Gupta and Kua 2019; Gupta *et al.* 2018]. Akthar *et al.* [2017] studied the effects of biochar as building material, the high water absorbing characteristics of biochar improved the mechanical strength and permeability of the concrete, in addition it accelerates the hydration of cement. Improving the porosity of concrete will improve the atmospheric contact area of the material, which tend to improve the CO<sub>2</sub> uptake of biochar concrete.

Iron ore tailing powder (ITP) is a waste generated in iron industry, for every 5 billion tons of iron production 80% of solid waste is generated [U.S Geological Survey 2020]. Many researchers identified the potential use of ITP as fine

aggregate, cement replacement admixture in concrete [Shettima *et al.* 2016; Gu *et al.* 2022; Han 2013; Zhang *et al.* 2021]. Up to 30% replacement of cement with ITP showed high pozzalonic characteristic even with lower w/c ratios [Osinubi *et al.* 2015]. The ultra-fine texture and irregular shape of ITP improved the hydration mechanism in the concrete. Huang *et al.* [Huang *et al.* 2013] experimentally proved that fine nature of ITP can potentially improve the ultimate strength of concrete due to the increase in its reactive contact area. The durability, sorptivity and permeability characteristics of concrete was improved with the addition of ITP in concrete, the uneven texture of ITP plays a major role in it [Al-khazaleh and Kumar 2023]. In order to improve the CO<sub>2</sub> uptake, by improving the permeability of the concrete, without affecting its strength, this research tends to utilize the mechanochemical characteristics of both the mineral admixtures biochar and ITP in the concrete.

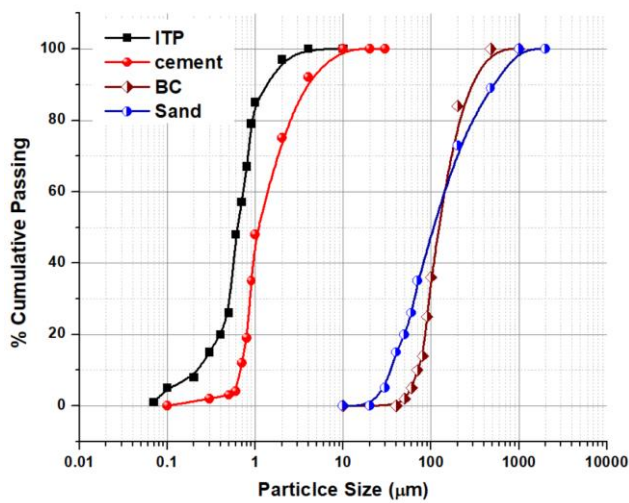


**Figure 1.** The particle size distribution of raw materials

The biochar produced from agricultural waste (particularly corn stover) was utilized in concrete manufacture. The fine aggregate was replaced with mechanically treated and untreated biochar at 0%, 5%, 10% and 15%. The untreated biochar has a high concentration of volatile organic compounds produced by slow pyrolysis process. Mechanical treatment of biochar involves heating the biochar in a muffle furnace at 600°C until it ignites, resulting in the formation of treated biochar. The cement in the concrete was replaced with ITP at 0%, 25% and 50% by the weight of cement. The primary objective of this research is to study the CO<sub>2</sub> sequestration potential of biochar concrete with ITP. In addition, the influence of biochar and ITP on strength, workability, and porosity characteristics of the concrete has to be determined.

## 2. Materials and mix proportion

The OPC 53-grade cement for the present study was supplied by Ramco Cement Limited, Tirunelveli, India. Crushed sand measuring up to 4.75 mm in size, with a specific gravity of 2.65 and a unit weight of 1640 kg/m<sup>3</sup> was used. Coarse aggregate with a maximum size of 19 mm was employed. The particle size classification of cement, aggregates and mineral admixtures was in accordance with

the specifications of IS 383:1970, as depicted in **Figure 1**. A water-to-cement ratio of 0.45 was uniformly used for all the mixtures. Conplast SP 430 a water-reducing chemical admixture was employed to improve the workability of the mix. The byproduct of the bioethanol industry was utilized in the production of biochar. Some examples of agricultural waste products in the bioethanol industry include bassage, rice husk, corn stover, palm shell, rubber wood, wheat straw and cow manure. In this research the biochar extracted from corn stover through the process of slow pyrolysis was utilized. During slow pyrolysis, the corn stovers is heated to a temperature of 550°C in a reactor without the presence of oxygen. Some of the previous studies indicate that 58% of the biomass will undergo slow pyrolysis and be transformed into high-quality biochar when corn stover is utilized [Wang *et al.* 2020]. The waste residues were subjected to heating in a metal kiln for a duration of two to three hours. The temperature during the synthesis of biochar increased at a rate of 30°C per minute. The biochar's quality is contingent upon its carbon content. The entire process of synthesizing biochar from corn stover was conducted in accordance with the previous literature [Delgado *et al.* 2013]. The slow pyrolysis process minimizes the gas condensation while heating. The untreated Biochar is referred to as BC1. This untreated biochar contains a high concentration of volatile organic compounds. Subsequently, the material is subjected to additional heating in a muffle furnace at a temperature of 600°C until it ignites, resulting in the formation of the treated biochar BC2. The heating process leads to the production of a significant amount of ash and decreases the presence of volatile compounds. The elemental characteristics of the samples prior to and following pre-treatment are displayed in the **Table 1**. The iron ore tailing powder was obtained from the iron ore mining industry located in Kanjamalai, Salem, India. **Table 2** displays the chemical composition of biochar, cement, ITP and Fine Aggregate (FA). The physical characteristics of cement, Biochar, iron ore tailings powder, and fine aggregate are shown in **Table 3**. The physical morphology of ITP and biochar were examined using SEM and shown in **Figure 2**. The XRD results shown in **Figure 3** of ITP indicate the presence of high amount of quartz (silica) mineral

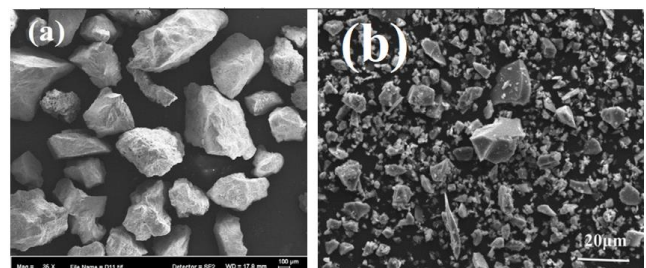


**Figure 2.** Morphology of (a) ITP and (b) Biochar

## 3. Mix Proportions

The conventional concrete mix proportions were established based on the guidelines specified in IS 10262:2009. **Table 3** presents the proportional distribution of the mix ratios that have been employed in mix preparation. The categorization of concrete formulations

was bifurcated into two primary classifications based on the type of biochar utilized. BC1 refers to the biochar that has not been treated, while BC2 refers to the biochar that has undergone treatment. Three series were formulated in each category according to the dosage of ITP. ITP was used as a cement substitute at 0%, 25%, and 50% of its weight. The computed quantity of ITP is combined with the overall quantity of superplasticizer and thoroughly blended prior to being dissolved in the determined volume of water. The prepared solution is introduced into the concrete mixer and agitated for an additional duration of three minutes. The method was employed to attain a consistent blend and even distribution of ITP within the concrete [Elkady *et al.* 2013]. The samples in each series of the concrete mixture were classified according to the quantity of biochar replacement. During the process of dry mixing, biochar is replaced with fine aggregate in the mixture at varying percentages: 0%, 5%, 10%, and 15%. The mechanical properties and CO<sub>2</sub> sequestration of admixture-modified concrete were assessed by casting and examining nine cubes measuring 150×150×150 mm, as well as three prisms measuring 40×40×160 mm for each mix designation. Thus, 216 cubes and 72 prisms were cast in total.

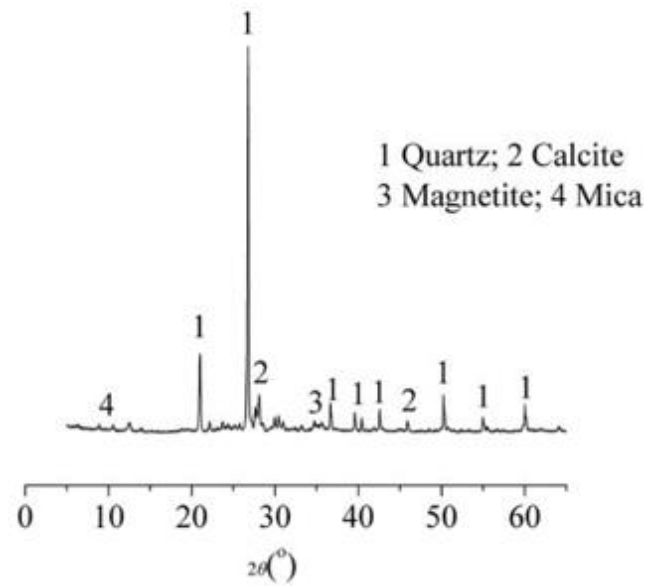


Figure 3. XRD of ITP

Table 1. Elemental characteristics of biochar before and after pretreatment

| Specimen ID | Volatile compounds | Bulk Density (kg/m <sup>3</sup> ) | C (%) | O(%)  | H(%) | N(%) |
|-------------|--------------------|-----------------------------------|-------|-------|------|------|
| BC 1        | 45.33              | 625                               | 63.2  | 13.24 | 4.25 | 6.58 |
| BC 2        | 20.21              | 556                               | 60.52 | 14.12 | 3.25 | 6.12 |

Table 2. Chemical composition of raw materials

|         | SiO <sub>2</sub> | Al <sub>2</sub> O <sub>3</sub> | Fe <sub>2</sub> O <sub>3</sub> | K <sub>2</sub> O | CaO   | MgO  | P <sub>2</sub> O <sub>5</sub> | MnO  | SO <sub>3</sub> | Na <sub>2</sub> O | BaO | CaO  | LOI  | Others |
|---------|------------------|--------------------------------|--------------------------------|------------------|-------|------|-------------------------------|------|-----------------|-------------------|-----|------|------|--------|
| OPC     | 21.11            | 4.15                           | 3.33                           |                  | 62.14 | 2.47 |                               |      | 2.94            | 0.54              |     | 0.84 | 2.1  | 0.38   |
| ITP     | 67.23            | 8.54                           | 8.86                           |                  | 3.64  | 4.85 |                               |      | 0.44            | 2.94              |     |      | 2.44 | 1.06   |
| Biochar | 4.12             |                                |                                | 19.15            | 60.12 | 6.12 | 4.17                          | 2.15 | 0.98            | 0.42              | 0.2 |      | 2.57 |        |
| FA      | 93.12            | 1                              | 0.5                            |                  | 0.4   |      |                               |      | 0.5             |                   |     |      | 3.8  |        |

Table 3. Physical properties of raw materials

|                  | D <sub>10</sub> | D <sub>50</sub> | D <sub>90</sub> | water absorption | Specific Gravity | Fineness Modulus |
|------------------|-----------------|-----------------|-----------------|------------------|------------------|------------------|
| Cement           | 2.56            | 4.32            | 6.92            | -                | 3.12             | 3.1              |
| ITP              | 0.2             | 0.68            | 1.08            | -                | 2.48             | 2.85             |
| BC               | 30              | 100             | 200             | -                | 3.5              | 3.15             |
| Fine Aggregate   | 30              | 70              | 475             | 1.98             | 2.58             | 3.4              |
| Coarse Aggregate | -               | -               | 19              | 0.66             | 2.69             | -                |

#### 4. Test / Experimentations

The workability of conventional and admixture-modified concrete was evaluated by performing a slump cone test in accordance with ASTM C143. A constant water to binder ratio of 0.45 was maintained for all the mixes. The use of Conplast SP 430, a synthetic polymer-based superplasticizer, has been employed to sustain the slump of concrete. The dry density of the specimens was determined in accordance with the ASTM C567 standard. The compressive strength of 150-mm cube samples was assessed after a 28-day and 90-day curing period, in accordance with the ASTM C39 standard. The carbon dioxide (CO<sub>2</sub>) absorption in the concrete was quantified by establishing a carbonation chamber, as depicted in the Figure 4. A closed chamber containing concrete samples was filled with 100% concentrated CO<sub>2</sub> gas. The humidity

was kept at (70 ± 5) %, the temperature was kept as (20 ± 2) °C, and the carbonization time was 7 days. Subsequently, the masses of the samples before and after carbonization were measured, after the concrete samples were cured, they were stored in an airtight container to prevent any damage caused by atmospheric CO<sub>2</sub> exposure. The samples underwent CO<sub>2</sub> absorption testing 130 days after being cast. Weight increase under carbonization conditions was denoted as WI<sub>cb</sub>, kg/m<sup>3</sup>. In addition, the weight increase under control conditions (cubes exposed to air) is denoted as WI<sub>c</sub>, kg/m<sup>3</sup>. The difference of increase in the weight of the concrete is the amount of CO<sub>2</sub> absorbed, as denoted below.

$$\Delta W = WI_{cb} - WI_c$$

$$\% \text{ of CO}_2 \text{ absorption} = \frac{\Delta W}{\text{Actual Cube Weight}} \times 100$$

The experimental procedures were conducted in accordance with the methods described in the previous literature [Castellote *et al.* 2008]. The mercury intrusion porosimeter (MIP) was used to determine the pore size distribution and cumulative pore volume of the hardened paste that contained an optimal dosage of ITP and Biochar. The morphology of the optimal concrete mix was examined

using a scanning electron microscope (SEM) after 90 days of curing. Chemically bound water in the concrete was quantified using the equation as described in previous literatures [Han *et al.* 2019].

**Table 3.** Mix Proportions

| Biochar Type | Mix Series | Mix ID  | OPC (kg/m <sup>3</sup> ) | Biochar (kg/m <sup>3</sup> ) | ITP (kg/m <sup>3</sup> ) | Sand (kg/m <sup>3</sup> ) | CA (kg/m <sup>3</sup> ) | Water (kg/m <sup>3</sup> ) | SP (kg/m <sup>3</sup> ) |      |
|--------------|------------|---------|--------------------------|------------------------------|--------------------------|---------------------------|-------------------------|----------------------------|-------------------------|------|
| BC1          | 0 ITP      | BC1-0S  | 364                      | -                            | -                        | 552                       | 1105                    | 163.8                      | 4.24                    |      |
|              |            | BC1-5S  | 364                      | 27.6                         | -                        | 524.4                     | 1105                    | 163.8                      | 4.24                    |      |
|              |            | BC1-10S | 364                      | 55.2                         | -                        | 496.8                     | 1105                    | 163.8                      | 4.31                    |      |
|              |            | BC1-15S | 364                      | 82.8                         | -                        | 469.2                     | 1105                    | 163.8                      | 4.33                    |      |
|              | 25 ITP     | BC1-0S  | 273                      | -                            | 91                       | 552                       | 1105                    | 163.8                      | 4.31                    |      |
|              |            | BC1-5S  | 273                      | 27.6                         | 91                       | 524.4                     | 1105                    | 163.8                      | 4.32                    |      |
|              |            | BC1-10S | 273                      | 55.2                         | 91                       | 496.8                     | 1105                    | 163.8                      | 4.41                    |      |
|              |            | BC1-15S | 273                      | 82.8                         | 91                       | 469.2                     | 1105                    | 163.8                      | 4.48                    |      |
|              | 50 ITP     | BC1-0S  | 182                      | -                            | 182                      | 552                       | 1105                    | 163.8                      | 4.40                    |      |
|              |            | BC1-5S  | 182                      | 27.6                         | 182                      | 524.4                     | 1105                    | 163.8                      | 4.55                    |      |
|              |            | BC1-10S | 182                      | 55.2                         | 182                      | 496.8                     | 1105                    | 163.8                      | 4.67                    |      |
|              |            | BC1-15S | 182                      | 82.8                         | 182                      | 469.2                     | 1105                    | 163.8                      | 4.75                    |      |
|              | BC2        | 0 ITP   | BC2-0S                   | 364                          | -                        | -                         | 552                     | 1105                       | 163.8                   | 4.97 |
|              |            |         | BC2-5S                   | 364                          | 55.25                    | -                         | 524.4                   | 1105                       | 163.8                   | 5.21 |
|              |            |         | BC2-10S                  | 364                          | 110.5                    | -                         | 496.8                   | 1105                       | 163.8                   | 5.44 |
| BC2-15S      |            |         | 364                      | 165.75                       | -                        | 469.2                     | 1105                    | 163.8                      | 5.64                    |      |
| 25 ITP       |            | BC2-0S  | 273                      | -                            | 91                       | 552                       | 1105                    | 163.8                      | 5.12                    |      |
|              |            | BC2-5S  | 273                      | 55.25                        | 91                       | 524.4                     | 1105                    | 163.8                      | 5.33                    |      |
|              |            | BC2-10S | 273                      | 110.5                        | 91                       | 496.8                     | 1105                    | 163.8                      | 5.49                    |      |
|              |            | BC2-15S | 273                      | 165.75                       | 91                       | 469.2                     | 1105                    | 163.8                      | 5.63                    |      |
| 50 ITP       |            | BC2-0S  | 182                      | -                            | 182                      | 552                       | 1105                    | 163.8                      | 5.28                    |      |
|              |            | BC2-5S  | 182                      | 55.25                        | 182                      | 524.4                     | 1105                    | 163.8                      | 5.35                    |      |
|              |            | BC2-10S | 182                      | 110.5                        | 182                      | 496.8                     | 1105                    | 163.8                      | 5.41                    |      |
|              |            | BC2-15S | 182                      | 165.75                       | 182                      | 469.2                     | 1105                    | 163.8                      | 5.59                    |      |

$$w = \frac{w_1 - w_2 - w_i}{1 - w_i}$$

$$w_i = m_c \cdot w_c + m_{itp} \cdot w_{itp} + m_{bc} \cdot w_{bc} + m_{fa} \cdot w_{fa}$$

$w_1$  and  $w_2$  are the weight of the paste after heating to 80°C and 1000°C respectively.  $m_c$ ,  $m_{itp}$ ,  $m_{bc}$ ,  $m_{fa}$  are the mass of the fraction of cement, ITP, BC and fine aggregate respectively in % and  $w_c$ ,  $w_{itp}$ ,  $w_{bc}$  and  $w_{fa}$  are the corresponding loss on ignition expressed in %.

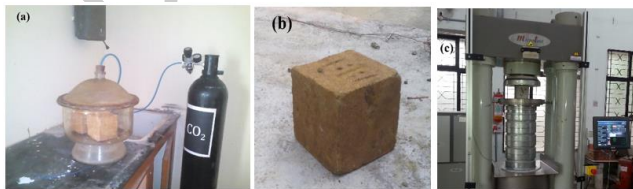


**Figure 4.** (a) CO<sub>2</sub> curing chamber (b) Carbonated cube (c) Compression strength test

## 5. Results and discussions

### 5.1. Dry density

The **Figure 5** illustrates the apparent density of the hardened admixture-modified concrete. In comparison to

the mixture containing pre-treated biochar BC1, the mixture containing treated biochar BC2 exhibited the lowest dry density. The bulk density of BC2 was 485 kg/m<sup>3</sup>, indicating a reduction of 8 to 12% compared to the bulk density of untreated biochar. The reduction in density of concrete has a negligible impact on its strength properties, rendering it most suitable for use as a lightweight building material. In contrast, the maximum density reduction observed was 5.82% in comparison to the control concrete. Despite substituting 50% of the cement with ITP, the BC2 mixture experienced a density reduction of 3.88%. It was observed that the brittle failure of the concrete becomes more severe as its density decreases during testing. A linear and gradual decrease in dry density signifies that the incorporation of biochar, whether in treated or untreated form, into the concrete mixture results in a reduction in dry density.

In a similar manner, the ITP marginally increases the density of the concrete. A 3% to 4% rise in dry density was observed as the dosage of ITP was increased. This suggests that the dry density of the concrete mixture remains unchanged when Biochar and ITP are incorporated as admixtures. The lowest dry density was 2430 kg/m<sup>3</sup> for the mix contains 15% BC2 and 0% ITP. The mix with 0% biochar

and 50% ITP showed a maximum density of 2577 kg/m<sup>3</sup>. The increase in density of the concrete due to the substitution of ITP can be attributed to the high apparent density of the ITP, as mentioned in previous research [Al-khazaleh and Kumar 2023].

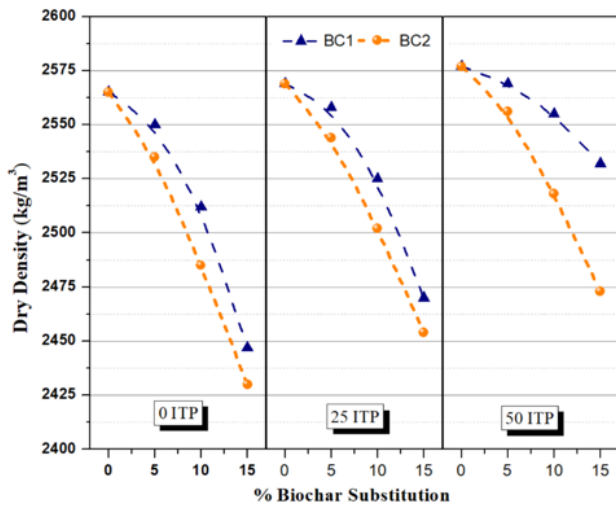


Figure 5. Dry density on biochar substitutions

## 5.2. Compressive Strength

The Figure 6 depicts the compressive strengths of all the concrete samples containing biochar and ITP at various dosages at 28 days and 90 days. Control concrete exhibited a compressive strength of 27.25 MPa after 90 days of water curing. The minimum compressive strength requirement for residential concrete, as specified by the code of practice, is 17 MPa.

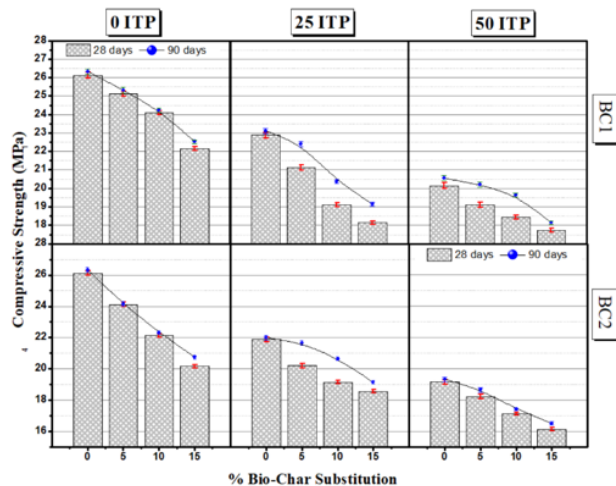


Figure 6. Effect of compressive strength on biochar substitutions

The incorporation of biochar in the concrete mixture resulted in a marginal reduction in compressive strength. The 15% sand replacement with biochar BC1 in the concrete resulted in a reduction of the compressive strength to 22 MPa. With the same replacement percentage, the strength of mixture BC2 was diminished to 20 MPa. The decline in strength lacks an apparent trend. Heat-induced water loss from biochar decreased the adhesion of concrete, leading to a reduction in its strength. When cement was substituted for ITP in the mixture, additional reduction was observed. The BC2 mix yielded a low of 16.5 MPa on 50% ITP substitution, making it

unsuitable for use in residential construction. However, with the addition of biochar and 25% ITP, the strength increased with age. The pozzolanic property of the ITP, as documented in prior literature, accounts for this [Yellishetty *et al.* 2008; Hou 2014; Goyal *et al.* 2015]. The percentage reduction in mix strength at 0%, 25%, and 50% ITP was 15.38%, 14.66%, and 12.19%, respectively. This demonstrates that the incorporation of ITP in biochar concrete mitigates the decrease in strength. In the same way, the rates of strength reduction for BC2 at 0%, 25%, and 50% ITP were 19.17%, 13.77%, and 12.25%, respectively. The rate of reduction is significantly lower in BC1 in comparison to BC2. The cause of this enormous rate of reduction is unclear. Nonetheless, both BC1 and BC2 mixtures demonstrated that the combination of ITP and biochar in the mix prevented a decline in the strength of the concrete. The relation between the dry density and compressive strength were shown in figure The test results and corresponding R<sup>2</sup> values proved that compressive strength drops with the reduction of density of the concrete. Hence, addition of ITP with Biochar proved to be a useful admixture in terms of improving or maintaining the strength of the biochar concrete. Interestingly the mix with 25% ITP showed higher strength at lower density comparatively. Specifically for BC2 concrete mix the strength attainment was higher than BC1. This was attributed to the optimal amount of ITP involving in the pozzolanic activity and the filler effect of BC2. Higher the admixture dosage agglomeration or improper dispersion may occur resulting in reduction of strength.

## 5.3. Strength activity index

The strength activity index of the admixture-modified concrete is shown in Figure 7. The SAI values showed a downtrend with addition of Biochar. It was very clear that addition of biochar in the concrete reduces the strength of concrete. However, BC1 and BC 2 substitution up to 10% with 0% and 25% ITP has SAI higher than 75% making the admixtures used to be pozzolanic. BC1 has higher SAI compared to BC2. Relatively lesser difference was noted between BC1 and BC2 when 25% ITP was substituted. This clarifies the combination of BC2 with ITP has considerably more advantageous in terms of strength aspects with respect to admixture dosage.

## 5.4. CO<sub>2</sub> uptake

Figure 8. Illustrates the carbon capture ability of biochar modified concrete samples with various ITP substitutions after being tested as per GB/T 50082:2009 using a carbonation test apparatus. The increase in mass ( $\Delta$ WL) with respect to sample volume increases with the concentration of biochar in the mix. In addition, the ITP substitution also improved the carbon absorption capacity of concrete. The increase in carbon absorption with ITP dosage is highly unclear. As per the previous studies the presence of rich source of Fe/Si minerals in ITP enhances the arbuscular mycorrhizal symbiosis, this arbuscular mycorrhizal fungi has the property of sequestering organic carbon and nitrogen [Li *et al.* 2024]. The maximum increase in mass was noted to be 23 g in terms of BC1 and 27.5 g for BC2. This showed the pre-treated biochar has high carbon

absorption property compared to the untreated biochar. The mass reduction during water lost during exothermic reaction is not accounted.

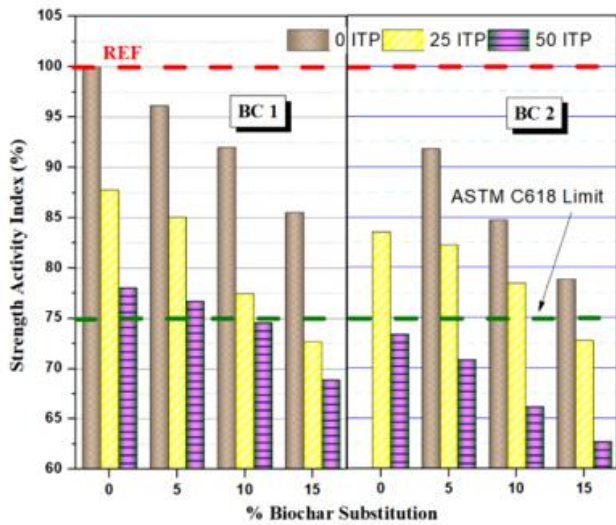


**Figure 7.** Relationship between Strength Activity Index and Biochar substitutions

According to literatures the percentage of weight gained is directly proportion to the carbon sequestration of the concrete [Castellote *et al.* 2008; He *et al.* 2024]. **Figure 9** depicts carbon absorption percentage with respect to biochar substitution dosage and ITP substitutions. The obtained regression values indicate there exist a linear relationship between percentage of biochar substitution and percentage of carbon absorption. Compared to control concrete BC2 mix with 0% ITP exhibited 150% higher carbon absorption. The rate of increase in CO<sub>2</sub> absorption BC1 was higher compared to BC2 concrete.

### 5.5. Bound water content

The bound water content of the hardened concrete containing biochar and ITP is depicted in the **Figure 10**. The bound water content is reduced as the cement content in the mix was reduced. Hydration products formation are higher during the initial days when water content in the mix is in adequate level. As the cement content in the mix is replaced by ITP, the bound water content is reduced. In addition, the biochar concentration in the mix allows water loss on heating. When the cement in the mix is not replaced, the water lost for BC1 and BC2 concrete was 5% and 20% by the weight of concrete respectively. The percentage loss of bound water is increased with the combination of BC2 and 50% ITP. This clearly indicates that less amount of hydration takes place in the mix due to the lack of cement, as a result bound water in the mix was lost. The preheated biochar absorbs the water in the matrix resulting in inadequate water available for hydration. This phenomenon showed maximum reduction in strength, dry density and bound water loss. The test results were accordance with the test findings in previous literatures [Li *et al.* 2010; Yang *et al.* 2024].

### 5.6. Pore volume

To investigate the reason for increase in CO<sub>2</sub> absorption characteristics of concrete three samples were subjected to mercury intrusion porosimetry test. The test results

were compared among the control concrete, BC1-15S with 25% ITP and BC2-15S with 50% ITP; as these mixes showed second and third highest CO<sub>2</sub> absorption characteristics. **Figure 11** depicts the differential pore size for the three samples. The pore sizes varied from 10 nm to 200 nm. Biochar in the concrete increased the smaller sized pores compared to the control concrete. The high water holding capacity of the biochar absorbs the water in the mix, creating water demand in the mix, as a result micro voids formed. Few of the micro voids are interlinked improving the tortuosity of the concrete. Allowing maximum area of the concrete exposed to CO<sub>2</sub> absorption. In addition the amount of hydration products improves the quantity of pore volume due to low water to binder ratio at the initial stage of hardened concrete [Wang *et al.* 2013].

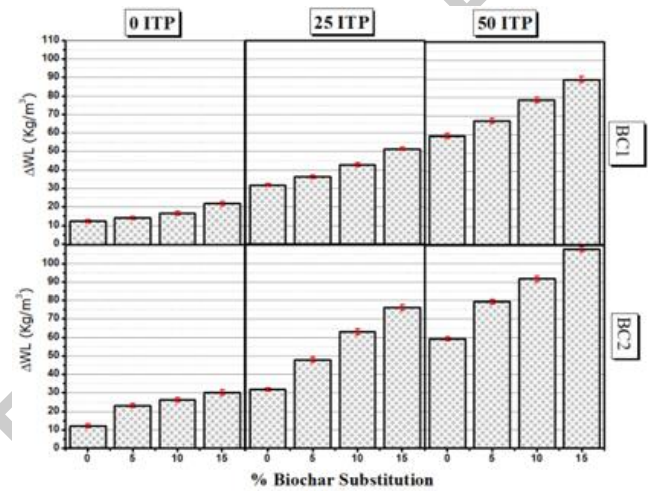


**Figure 8.** CO<sub>2</sub> sequestration

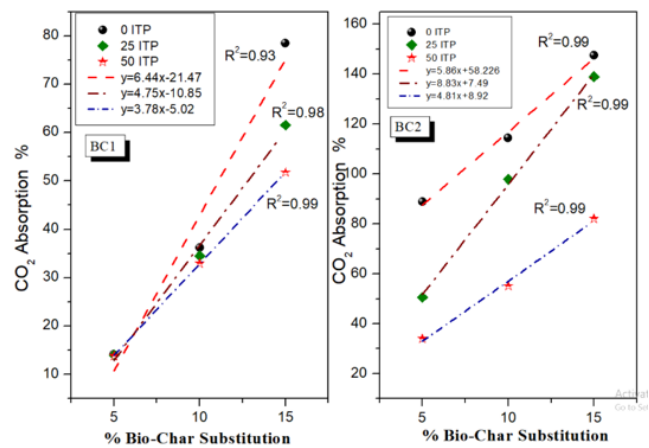


**Figure 9.** Percentage of CO<sub>2</sub> uptake on biochar substitutions

The porosity of the concrete gets reduced as a result of carbonation. **Figure 12** depicts the total porosity of the three concrete samples before and after carbonation. As the differential pore volume is higher for BC1-15S and BC2-15S the porosity values were proportionally higher. The increase in the difference in porosity after carbonation indicates the presence of mineral admixtures biochar and ITP in the concrete improves the CO<sub>2</sub> sequestration ability of the concrete.

### 5.7. SEM Analysis

The **Figure 13** (a) and (b) shows the SEM images of the optimum mixes BC1-15S and BC2-15S. It was very evident

that high pores are noticed in BC1-15S mix comparatively. Large amount of ettringite (needle like structure) are visible inside the pores. The hydration products are higher with BC2-15S. This indicate the reaction of binder with ITP is higher at this optimal dose. The substitution of biochar and iron powder undergo pozzolanic reaction to form additional CSH gel. The SEM image findings are consistent with the experimental test results conducted. The use of treated biochar improves the pores in the concrete, which is evident in the SEM images. As a result the CO<sub>2</sub> value increases.

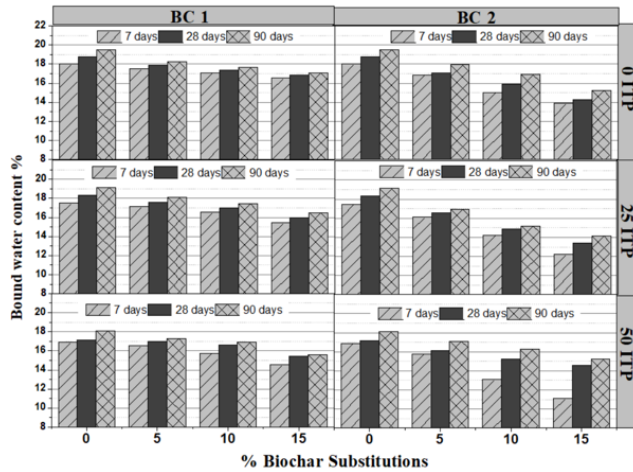


Figure 10. Bound water content and biochar substitutions

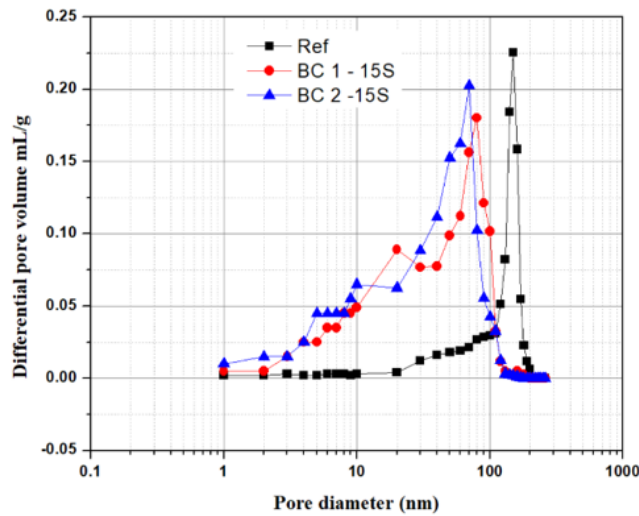


Figure 11. Differential pore volume and pore diameter

### 6. Conclusions

The test results obtained by substituting the fine aggregate with biochar and cement in the concrete containing Iron Ore Tailing Powder (ITP) led to the following findings.

The dry density of hardened concrete reduces as the amount of biochar concentration increases. When up to 6% of treated biochar is utilised, a decline in density of the concrete is seen compared to control concrete. The compressive strength of concrete is influenced by its density, which is why a decrease in compression strength was seen. The combination of biochar and ITP in concrete effectively prevents a decrease in density and strength of the material.

The mechanical bonding of ITP and biochar in the concrete was demonstrated by a higher strength to density ratio. The concrete exhibited its highest strength when 25% ITP was used as cement substitution for BC1-15S and BC2-15S. This demonstrates that the optimal dose of admixtures resulted in improved particle packing and increased pozzolanic reactivity.

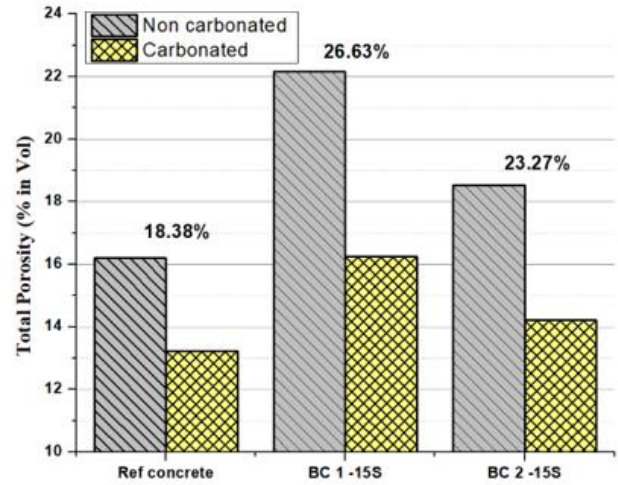


Figure 12. Total porosity

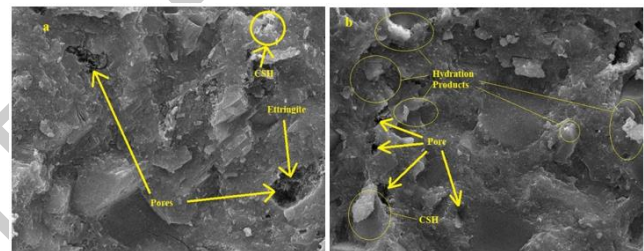


Figure 13. (a) SEM image of optimal mix BC1-15S (b) SEM image of optimal mix BC2-15S

The highest absorption of CO<sub>2</sub> occurs when biochar is used. The impact of ITP on CO<sub>2</sub> sequestration is negligible. The processed biochar has the highest capacity for CO<sub>2</sub> absorption.

The use of biochar and ITP in concrete enhances porosity by generating small spaces, so increasing the surface area of interaction between the concrete and the atmosphere. Consequently, the value of CO<sub>2</sub> absorption was enhanced.

Therefore, the use of innovative waste items in concrete to produce environmentally friendly building materials is paving the way for sustainable construction methods. By replacing 15% of the fine aggregate with biochar and using 25% ITP as a cement substitute in the concrete, a significant reduction in the consumption of raw materials may be achieved. However, further investigation is required to examine the durability characteristics of biochar-modified concrete.

### References

Ahmad S., Khushnood R. A., Jagdale P., Tulliani J.-M. and Ferro G. A. (2015). "High performance self-consolidating cementitious composites by using micro carbonized bamboo particles," *Materials & Design*, vol. 76, pp. 223–229, doi: <https://doi.org/10.1016/j.matdes.2015.03.048>.

- Akhtar A. and Sarmah A. K. (2018). "Novel biochar-concrete composites: Manufacturing, characterization and evaluation of the mechanical properties," *Science of The Total Environment*, vol. 616–617, pp. 408–416, doi: 10.1016/j.scitotenv.2017.10.319.
- Al Khazaleh M., Kumar P. K., Mohamed M. J. S., and Kandasamy A. (2022). "Influence of coarse coal gangue aggregates on properties of structural concrete with nano silica," *Materials Today: Proceedings*, no. xxxx, doi: 10.1016/j.matpr.2022.08.188.
- Al-khazaleh M. and Kumar P. K. (2023). "Optimization Studies of Iron Ore Tailings Powder and Natural Zeolite as Concrete Admixtures," vol. 9, no. 12, pp. 3075–3091.
- Aprianti E., Shafiq P., Bahri S., and Farahani J. N. (2015). "Supplementary cementitious materials origin from agricultural wastes – A review," *Construction and Building Materials*, vol. 74, pp. 176–187, doi: <https://doi.org/10.1016/j.conbuildmat.2014.10.010>.
- Castellote M., Andrade C., Turrillas X., Campo J., and Cuello G. J. (2008). "Accelerated carbonation of cement pastes in situ monitored by neutron diffraction," *Cement and Concrete Research*, vol. 38, no. 12, pp. 1365–1373, doi: 10.1016/j.cemconres.2008.07.002.
- Delgado R., Rosas J. G., Gómez N., Martínez O., Sanchez M. E., and Cara J. (2013). "Energy valorisation of crude glycerol and corn straw by means of slow co-pyrolysis: Production and characterisation of gas, char and bio-oil," *Fuel*, vol. 112, pp. 31–37, doi: 10.1016/j.fuel.2013.05.005.
- Elkady H., Serag M., and Elfeky M. (2013). "Effect of Nano Silica De-agglomeration, and Methods of Adding Super-plasticizer on the Compressive Strength, and Workability of Nano Silica Concrete," *Civil & Environmental*, vol. 3, no. 2, pp. 21–35, [Online]. Available: <http://search.ebscohost.com/login.aspx?direct=true&profile=ehost&scope=site&authtype=crawler&jrnl=22250514&AN=88998269&h=WUbt+pmz0hOlspFrWCy6dsEmS9SgbmvWg/stBu17WqGTSxEc3syzqOxhT5HzBLZaWey2R9OXaXsnmmZbB9sXA==&crl=c>
- Goyal S., Singh K., Hussain A., and Singh P. R. (2015). "Study on partial replacement of sand with iron ore tailing on compressive strength of concrete," *International Journal of Advanced Engineering and Technology*, vol. 3, no. 2, pp. 243–248.
- Gu X., Zhang W., Zhang X., Li X., and Qiu J. (2022). "Hydration characteristics investigation of iron tailings blended ultra high performance concrete: The effects of mechanical activation and iron tailings content," *Journal of Building Engineering*, vol. 45, p. 103459, doi: <https://doi.org/10.1016/j.jobe.2021.103459>.
- Gupta S. and Kua H. W. (2019). "Carbonaceous micro-filler for cement: Effect of particle size and dosage of biochar on fresh and hardened properties of cement mortar," *Science of The Total Environment*, vol. 662, pp. 952–962, doi: <https://doi.org/10.1016/j.scitotenv.2019.01.269>.
- Gupta S., Kua H. W., and Low C. Y. (2018). "Use of biochar as carbon sequestering additive in cement mortar," *Cement and Concrete Composites*, vol. 87, pp. 110–129, 2018, doi: 10.1016/j.cemconcomp.2017.12.009.
- Gupta S., Kua H. W., and Pang S. D. (2018). "Biochar-mortar composite: Manufacturing, evaluation of physical properties and economic viability," *Construction and Building Materials*, vol. 167, pp. 874–889, doi: <https://doi.org/10.1016/j.conbuildmat.2018.02.104>.
- Han F., Song S., Liu J., and Huang S. (2019). "Properties of steam-cured precast concrete containing iron tailing powder," *Powder Technology*, vol. 345, pp. 292–299, doi: 10.1016/j.powtec.2019.01.007.
- Han P. (2013). "Experimental Study on High Silicon Iron Ore Tailings Effect on Concrete Workability and Compressive Strength," *Northeast Univ. Boston, MA, USA*.
- He X. et al. (2024). "Wet grinding carbonation technique: Achieving rapid carbon mineralization of concrete slurry waste under low CO2 flow rate," *Chem. Eng. J.*, vol. 493, p. 152836, doi: <https://doi.org/10.1016/j.cej.2024.152836>.
- Hou Y. (2014). "Comparison of effect of iron tailing sand and natural sand on concrete properties," *Key Engineering Materials*, vol. 599, pp. 11–14, doi: 10.4028/www.scientific.net/KEM.599.11.
- Huang X., Ranade R., Ni W., and Li V. C. (2013). "Development of green engineered cementitious composites using iron ore tailings as aggregates," *Constr. Build. Mater.*, vol. 44, pp. 757–764, doi: 10.1016/j.conbuildmat.2013.03.088.
- Kua H. W., Pedapati C., Lee R. V., and Kawi S. (2019). "Effect of indoor contamination on carbon dioxide adsorption of wood-based biochar – Lessons for direct air capture," *Journal of Cleaner Production*, vol. 210, pp. 860–871, doi: <https://doi.org/10.1016/j.jclepro.2018.10.206>.
- Li C., Sun H., Yi Z., and Li L. (2010). "Innovative methodology for comprehensive utilization of iron ore tailings. Part 2: The residues after iron recovery from iron ore tailings to prepare cementitious material," *Journal of Hazardous Materials*, vol. 174, no. 1–3, pp. 78–83, doi: 10.1016/j.jhazmat.2009.09.019.
- Li Z. et al. (April, 2022). "Plant biomass amendment regulates arbuscular mycorrhizal role in organic carbon and nitrogen sequestration in eco-engineered iron ore tailings," *Geoderma*, vol. 428, no. , doi: 10.1016/j.geoderma.2022.116178.
- Osinubi K. J., Yohanna P., and Eberemu A. O. (2015). "Cement modification of tropical black clay using iron ore tailings as admixture," *Transportation Geotechnics*, vol. 5, pp. 35–49, doi: <https://doi.org/10.1016/j.trgeo.2015.10.001>.
- Palaniappan K. K., Komarasamy C., and Murugan S. (2022). "Utilization of Cuttlebone as Filler in Hydrophobic Foam Mortar: A Technical and Economical Feasibility Study," *Journal of Materials in Civil Engineering*, vol. 34, no. 8, pp. 1–14, doi: 10.1061/(asce)mt.1943-5533.0004335.
- Restuccia L., Reggio A., Ferro G. A. and Kamranirad R. (2017). "Fractal analysis of crack paths into innovative carbon-based cementitious composites," *Theoretical and Applied Fracture Mechanics*, vol. 90, pp. 133–141, doi: <https://doi.org/10.1016/j.tafmec.2017.03.016>.
- Roberts K. G., Gloy B. A., Joseph S., Scott N. R., and Lehmann J. (Jan. 2010). "Life Cycle Assessment of Biochar Systems: Estimating the Energetic, Economic, and Climate Change Potential," *Environmental Science & Technology*, vol. 44, no. 2, pp. 827–833, doi: 10.1021/es902266r.
- Shettima A. U., Hussin M. W., Ahmad Y., and Mirza J. (2016). "Evaluation of iron ore tailings as replacement for fine aggregate in concrete," *Construction and Building Materials*, vol. 120, pp. 72–79, doi: 10.1016/j.conbuildmat.2016.05.095.
- U.S Geological Survey, "Iron ore 2020," *U.S. Geol. Surv. Miner. Comm. Summ.*, vol. 1, no. 703, pp. 88–89, 2020, [Online]. Available: <https://pubs.usgs.gov/periodicals/mcs2020/mcs2020-iron-ore.pdf>



- Wang D., Jiang P., Zhang H., and Yuan W. (2020). "Biochar production and applications in agro and forestry systems: A review," *Science of The Total Environment*, vol. 723, p. 137775, doi: 10.1016/j.scitotenv.2020.137775.
- Wang Q., Yan P., Yang J., and Zhang B. (2013). "Influence of steel slag on mechanical properties and durability of concrete," *Construction and Building Materials*, vol. 47, pp. 1414–1420, doi: 10.1016/j.conbuildmat.2013.06.044.
- Xuan Mao L. *et al.* (2018). "Multi-phase modelling of electrochemical rehabilitation for ASR and chloride affected concrete composites," *Composite Structures*, vol. 207, no. August 2018, pp. 176–189, doi: 10.1016/j.compstruct.2018.09.063.
- Yang J. *et al.* (2024). "Achieving carbon utilization and storage (CUS) in cement-based materials with wet-grinding carbonated concrete slurry waste," *Cement and Concrete Composites*, vol. 152, p. 105642, doi: <https://doi.org/10.1016/j.cemconcomp.2024.105642>.
- Yellishetty M., Karpe V., Reddy E. H., Subhash K. N., and Ranjith P. G. (2008). "Reuse of iron ore mineral wastes in civil engineering constructions: A case study," *Resources, Conservation and Recycling*, vol. 52, no. 11, pp. 1283–1289, doi: 10.1016/j.resconrec.2008.07.007.
- Zhang N., Tang B., and Liu X. (2021). "Cementitious activity of iron ore tailing and its utilization in cementitious materials, bricks and concrete," *Construction and Building Materials*, vol. 288, p. 123022, doi: 10.1016/j.conbuildmat.2021.123022.

UNCORRECTED PROOFS